Intracluster Ion/Molecule Reactions within 1,1-Difluoroethylene Homocluster

Sun Young Lee, Chang Ju Choi, and Kyung-Hoon Jung*

Center for Molecular Science and Department of Chemistry, Korea Advanced Institute of Science and Technology, Taeduck Science Town, Taejon 305-701, Korea
Received November 18, 1996

The intracluster ion/molecule reactions within 1,1-difluoroethene homocluster have been studied by electron-impact quadrupole mass spectrometry. When CH_2CF_2 seeded in helium is expanded and ionized by electron impact, two different types of ion/molecule association (polymerization) reaction products, *i.e.*, $(CH_2CF_2)_n^+$ ($n \geq 1$) and $(CF_2CH_2)_qX^+$ (X=fragment species, $q \leq n$), are formed. The higher association products, $(CH_2CF_2)_n^+$ (n=3, 4), have shown stronger intensities over the lower association product, $(CH_2CF_2)_2^+$, in the low electron impact energy region (<39 eV). These stronger intensities are interpreted in terms of the stabilization of these ions due to the ring formations over the dimer ion in this energy region. The evidence of ring formation mechanism is on the basis of the intensity distribution of fragments at various electron impact energy. In another typical branched-chain growth reaction of these compounds, the F-shift reaction path is found to be more favorable energetically than the H-shift via the fragment patterns of clusters and semi-empirical calculation.

Introduction

The ion chemistry of olefins has been investigated extensively both in the gas and the condensed phases and found to be strongly dependent on the state of solvation.[1-3] In the gas phase, the reaction takes place in bimolecular between a single ion and a molecule, while in the condensed phase the olefin monomer induces the polymerization by interacting with the highly energized olefinic ions. Free cationic polymerization is a known process of reaction propagation in these systems.[4,5] Consequently, the study of these systems serves us for the understanding of a wide range of problems, including the mechanism of polymerization, nucleation on polymer molecules in the vapor phase, soot formation in hydrocarbon flames, and photoemission from polymeric ions generated from highly exothermic processes.

Since the clusters can serve in some degree as a microscopic model of solutions, a reagent molecule surrounded by solvent molecules, they can therefore make a link between the gas and condensed phases.[6-10] When the neutral cluster is ionized, three phenomena are observed such as the evaporation, fragmentation and reaction within the cluster. The intracluster ion/molecule reaction, a new class of chemical process, has no counterpart in gas phase bimolecular reactions.[11-15] Since product ions reflect the sequential reactions within ionized molecular clusters, their analysis gives chance to acquire the information on the polymerization mechanism and polymer molecular sizes involved in the processes.

In this work we report the intracluster ion/molecule reactions occurring within the solvated environments in 1,1-difluoroethene (1,1-DFE) homocluster. The 1,1-DFE molecule is a known monomer unit of an elastomer with thermal stability and chemical inertness.[16] The elastomer properties have been attributed to the presence of pendent CF_3 groups in the polymer. The 1,1-DFE is selected as a prototype molecule since it formes a neutral cluster easily owing to its high dipole moment.[4] The study of the intracluster ion/molecule reaction provides new information on the mechanism involved in the first stages of cationic polymerization of 1,1-DFE.

*Author to whom correspondence should be addressed.

Experimental

The experimental setup used in this work has been described in detail elsewhere.[17] A neutral cluster beam is generated using a 0.5 mm diameter pulsed nozzle in the source chamber, which is separated from the main chamber by a Cu electroformed conical skimmer with an orifice diameter of 1.2 mm. The skimmer is located 3 cm apart from the nozzle. The pressures in a source and main chamber are maintained lower than 1×10^{-5} and 5×10^{-6} torr, respectively.

The reaction products were analyzed using a quadrupole mass spectrometer, placed 36 cm down stream from the nozzle. The mass spectrometer (VG Quadrupoles Ltd., MSL-300D5TST2) consists of an electron impact ionizer (modified to variable electron energy, 10-100 eV), a triple mass filter and a channel electron multiplier (CEM). A homemade gate integration circuit has been used to obtain the clean pulsed signals from CEM detector by subtracting "background" noises. The time delay for gate integration is set 400 (s after the molecular beam valve firing at the gate width of 1 ms. The output signal from the gate integrator is sent to the digital multimeter (Iwatsu Model SC-7403) coupled with a PC (NEC PC-9801VM). The mass spectra typically are accumulated for 20 pulses per mass.

1,1-difluoroethene (PCR Research, stated purity 99%) and helium (Jung-ang Argon Co., stated purity 99.99%) are used without further purification.

Results and Discussion

Figure 1 shows a typical mass spectrum of 2% 1,1-DFE seeded in 6.5 atm He expansion at 70 eV electron impact

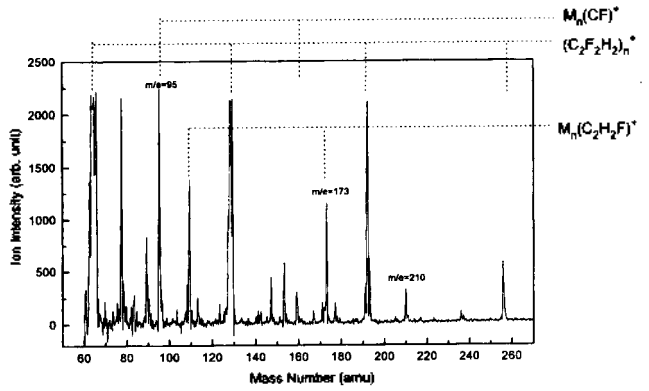

Figure 1. The mass spectrum of 2% 1,1-DFE seeded in 6.5 atm He expansion at 70 eV electron impact energy, M=$C_2H_2F_2$.

Table 1. The product ion series (M=$C_2F_2H_2$ monomer unit)

Ion Series	Mass (amu)	Product Ions	Loss radical series
1	77, 141, 205	$M_{1,2,3}CH^+$	CF_2H
2	78, 142, 206	$M_{1,2,3}CH_2^+$	CF_2
3	89, 153	$M_{1,2}C_2H^+$	HF_2
4	90, 154	$M_{1,2}C_2H_2^+$	F_2
5	83, 147, 211	$M_{1,2,3}F^+$	C_2H_2F
6	95, 159, 223	$M_{1,2,3}CF^+$	CH_2F
7	108, 172	$M_{1,2}C_2HF^+$	HF
8	109, 173	$M_{1,2}C_2H_2F^+$	F
9	114, 178	$M_{1,2}CF_2^+$	CH_3
10	115, 179	$M_{1,2}CF_2H^+$	CH
11	127, 191, 255	$M_{1,2,3}C_2HF_2^+$	H
12	69	CF_3^+	C_3H_4F
13	82, 146, 210	$M_{0,1,2}C_2HF_3^+$	C_2H_3F
14	39, 103, 167	$M_{0,1,2}C_3H_3^+$	CHF_4
15	59	$C_3H_4F^+$	CF_3
16	129, 193, 257	$M_{2,3,4}H^+$	C_2HF_2
17	113	$C_3HF_4^+$	CH_3
18	57	$C_4H_9^+$	

energy. A series of clusters of the form $[(C_2H_2F_2)_nX]^+$ ($n \geq 1$, X=a fragment from the ion/molecule reaction) are observed in 1,1-DFE homocluster system. All the ion peaks are assigned and listed in Table 1. Most of these products are formed by a chain- or stepwise-polymerization-like reactions which have not been observed in the gas phase free ion/molecule reactions. Protonated cluster ions and $[(C_2F_2H_2)_nC_2HF_2]^+$ produced by losing H atoms from parent molecular ions are also observed.

The peak intensities of mass spectrum in cluster ion series decrease in general with increasing the cluster size. In the 1,1-DFE system, however, the relative intensities of ion series of the dimer are different from those of the trimer and tetramer. The major fragment peaks of dimer are produced by losing CH_xF_y radical ($x+y \leq 3$) from the parent ion, while the major fragment peaks of trimer and tetramer are formed by losing H_xF_y ($x+y \leq 2$) radicals from the parent molecular ions. As a consequence, the base peak of the dimer ($[(C_2H_2F_2)CF]^+$, m/z=95) is produced by losing CH_2F radical from the parent ion, while that of the trimer ($[(C_2H_2F_2)_2C_2H_2F]^+$, m/z=173) is formed by losing F atom.

In the ethene cluster system, a study[18,19] has shown that the relative intensities of fragment ion series such as $[(C_2H_4)_nC_3H_5^+]/[(C_2H_4)_nC_4H_7^+]$ remains constant with the increase of n. A cationic polymerization study[1,4] has revealed that both the 1,1-DFE and ethene clusters have shown the magic number of n=4, expecting the similar structures and ion/molecule reaction mechanism between both clusters. The reaction scheme, suggested for ethene clusters[4] consists of three possible reaction paths, *i.e.*, the chain propagation, the hydride shifts, and the ring formation. Hydride shift reactions are suggested on the basis of no observed primary carbocations as reaction intermediates in solution.

Table 2. The structures of dimer calculated by PM3 method

No.	Structures	ΔH_f (kcal/mol)
I	$[CF_2\text{-}CH_2\text{-}CF_2\text{-}CH_2]^+$	68.98
II	$[CF_2\text{-}CH_2\text{-}CH_2\text{-}CF_2]^+$	53.91
III	$[CH_2\text{-}CF_2\text{-}CF_2\text{-}CH_2]^+$	80.38
IV	$[CF_2\text{-}CH_2\text{-}CF\text{-}CH_2F]^+$	60.19
V	$[CF_2H\text{-}CH\text{-}CF_2\text{-}CH_2]^+$	89.37
VI	$[CF_2H\text{-}CH\text{-}CH_2\text{-}CF_2]^+$	58.81

Structural determination of dimer ion and F-shift reactions. The structural study of the dimer has been made by observing the fragment patterns to show the typical ion/molecule reactions within the 1,1-DFE cluster ions. The formation of $[(C_2F_2H_2)CF]^+$ (m/z=95), the base peak of the dimer, is examined to obtain the structural information of the dimer from neutral fragments lost in forming the high mass peaks. The $[(C_2H_2F_2)CF]^+$ is formed by the loss of CH_2F from the $(C_2H_2F_2)_2^+$ parent ions. Among the possible structures of dimers, the structure IV in Table 2 can only afford the loss of CH_2F radical through the α-cleavage. Accordingly, the formation of structure IV from $(CF_2CH_2)_2^+$ needs to be studied to explain the formation of $[(C_2F_2H_2)CF]^+$. Three possible structures, *i.e.*, the structures I, II and III in Table 2 are the possible candidates for the $(CF_2CH_2)_2^+$. Structure III is excluded since its heat of formation is much higher than the others as shown in Table 2. In addition, no possible path to structure IV is found from structure II. On the contrary, the structure I gives structure IV through F-shifts and structure V is formed through H-shifts from structure I. This is an experimental evidence that the F-shift plays an important role in 1,1-DFE cluster, indicating simultaneously that structure I is most likely an intermediate. These reasonings are also supported by the heat of formation calculation *via* PM3 method.

Hydride shifts in ethylene dimer ions are calculated using the PM3 semi empirical method[20] in the MOPAC93 package[21] and found that the primary ions rearrange rapidly *via* the shifts into the energetically more stable secondary cations as,

$$\underset{\Delta H_f=249.5 \text{ kcal mol}^{-1}}{[CH_2\text{-}CH_2\text{-}CH_2\text{-}CH_2]^+} \longrightarrow \underset{230.65 \text{ kcal mol}^{-1}}{[CH_2\text{-}CH_2\text{-}CH\text{-}CH_3]^+}$$

Secondary cation is found to be more stable than that of a primary cation by *ca* 18.8 kcal mol^{-1} and is consistent with the observation. In the calculation of the 1,1-DFE cluster system, the structure IV, F-shifted, is the energetically more stable than the structure I but the structure V, H-shifted, is not, from the PM3 calculation[21] in Table 2. In ad-

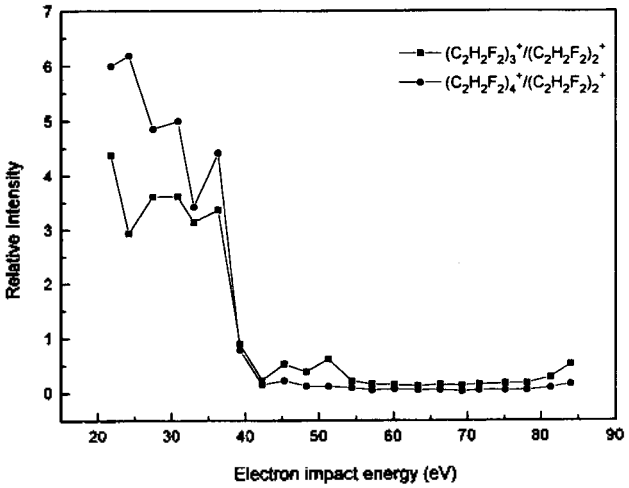

Figure 2. Relative intensity of the $(C_2H_2F_2)_n^+$ (n=3, 4) to the $(C_2H_2F_2)_2^+$ depending on the electron impact energy.

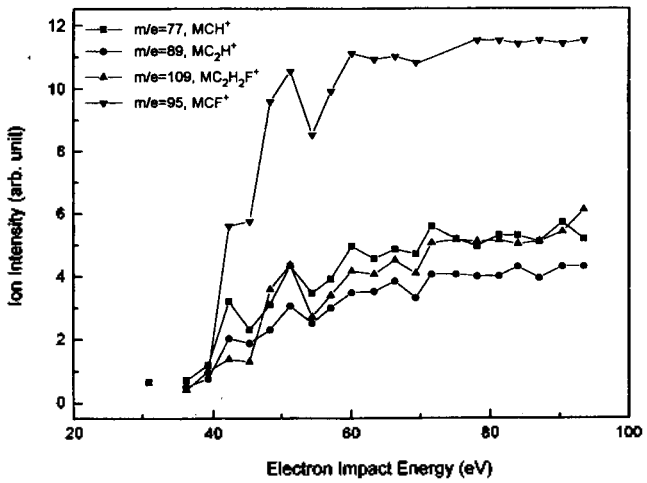

Figure 3. The intensities of the fragment ions as a function of the electron impact energy in the dimer, M=$C_2H_2F_2$.

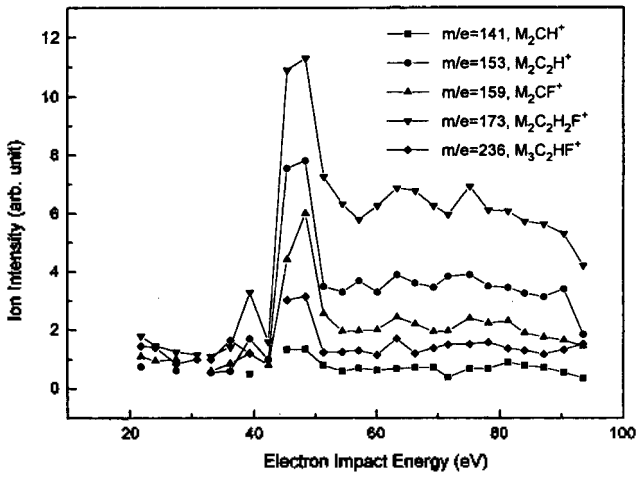

Figure 4. The intensity of the fragment ions as a function of the electron impact energy in the trimer and tetramer, M=$C_2H_2F_2$.

dition, the mass peaks produced from the structures IV and V through the α-cleavages are $C_2H_2F_2CF^+$ (m/z=95) and $C_2H_2F_2CH^+$ (m/z=77), respectively, and the former is the more intensive than the later. Based on the consistencies of calculated and experimental results discussed above, we propose that the F-shift reaction is the preferable process than the H-shift in CH_2CF_2-cluster ions.

Another evidence of the preference of the structure I over the structure II is discussed in terms of the intrinsic difference between the free and intracluster ion/molecule reactions. In the free ion/molecule reaction,[22] the base peak for the dimer is $[C_2F_2H_2(CH)]^+$ m/z=77 which is formed by an addition reaction of CH_2F^+ (m/z=33) to 1,1-DFE molecule by,

$$CH_2F^+ \text{ (m/z=33)} + C_2F_2H_2 \rightarrow C_3H_3F_2^+ \text{ (m/z=77)} + HF$$

On the other hand, $[(C_2F_2H_2)CF]^+$ peak (m/z=95) has only been detected at high conversion condition, where the dimer parent ions are easily formed due to high concentration of the monomers. These fragmentation patterns are not found in the case of 1,1-DFE intracluster ion/molecule reaction. These intrinsic differences between the free and 1,1-DFE intracluster ion/molecule reactions may be due to the solvation effect in the clusters. Neutral clusters, comprising van der Waals bonded constituents via the dipole-dipole interaction, may undergo the evaporative dissociation or the ionization by electron impact and then the intracluster process follows. Since molecular tumbling in the cluster is not as easy as in the isolated gas phase, the resultant ion retains the same structural configuration of the neutral molecule as the sequence of the structure I.

Stability of tetramer ions. The stability of the tetramer ion has been studied by observing the electron impact energy dependence of the intensity of cluster ions. Figure 2 shows the variation of the relative intensity of $(C_2H_2F_2)_n^+$ (n=3, 4) to $(C_2H_2F_2)_2^+$ cluster ions as a function of electron impact energy. The relative intensity is unity at 39 eV and increases rapidly as energy decreases. This finding is more prominent in the tetramer ion. The average cluster size increases with decrease in electron impact energy because of the less evaporation from the abundant cluster ion. As seen in Figure 2, the tetramer ion exhibits six folds higher intensity comparing with the dimer ion in lower energy range, owing to its particular stability. This is well demonstrated by the previous workers.[1,4] They have suggested that the stability of the tetramer ion is related to the formation of cyclic ions with low ring strain energy that serves as an energy trap in reaction sequence, but they were not able to provide any experimental evidence of ring formation.

Figures 3 and 4 illustrate the intensity distributions of major cluster ions, $[(C_2F_2H_2)_nX]^+$ (X=C_2H_2F, CF, C_2H,CH) of dimer, trimer, and tetramer, respectively. The peak intensities of these ions increase in the dimer with the electron impact energy increase up to 70 eV. This tendency is explained by the reaction paths such as evaporation, fragmentation and the intracluster ion/molecule reactions within the parent cluster ion $[(C_2F_2H_2)_q^+]^*$ with a large amount of excess energy. On the other hand, the energy dependence curves of the trimer and tetramer display the sharp maximum intense peaks at about 50 eV. This implies that the fragmentation requires some fixed amount of additional energies in the trimer and tetramer. This extra consumption of

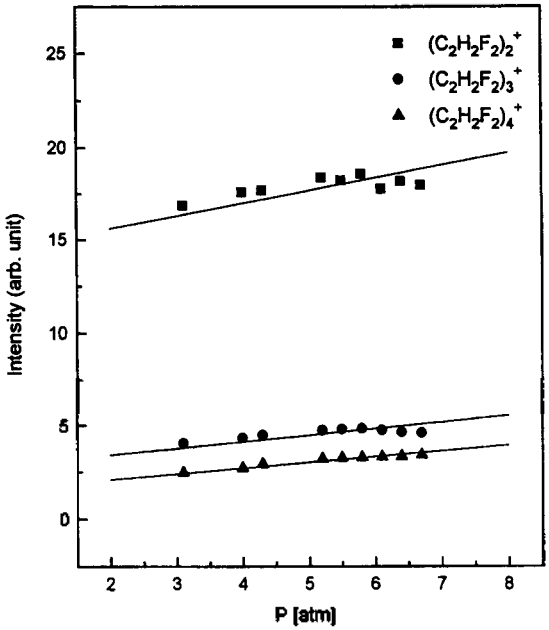

Figure 5. The stagnation pressure dependence of the $(C_2H_2F_2)_n^+$ (n=2, 3, 4) at 70 eV impact energy.

fixed amount of energy for the fragmentation may be interpreted as the ring opening process from the cyclic ring conformations of these cluster ions. Since the successive evaporation and fragmentation may proceed further after the ring opening process, the number densities of major fragments show sudden decrease just after 50 eV and then remain steady. The intensity distributions of these major ions as a function of electron impact energy are therefore considered as a direct evidence of the ring structures of trimer and tetramer ions.

Stagnation pressure dependence. Figure 5 shows the stagnation pressure dependence of the intensity of the $(C_2H_2F_2)_n^+$ (n=2-4) at 70 eV impact energy. The pressure dependences have shown that the slopes of the trimer and tetramer ions are almost equal while that of the dimer is two times larger. According to the scaling law,[23] the difference in the slope indicates that the dimer is not formed mainly *via* a monomer evaporation from the trimer ion.

The base peak of the tetramer, the $[(C_2H_2F_2)_nC_2HF_3]^+$ m/z= 210 (n=2), is stronger than those of m/z=82 (n=0) and m/z= 146 (n=1) peaks. The base peak can be formed either by the loss of the C_2H_3F radical from $(C_2H_2F_2)_4^+$ (m/z=256) or by the loss of C_2H_2F radical from $[(C_2H_2F_2)_3C_2HF_2]^+$ (m/z= 255). In order to obtain the information of the reaction pathways further, we have measured the pressure dependence of ion intensities at electron impact energy of 70 eV and displayed in Figure 6. The pressure dependence of $[(C_2H_2F_2)_2C_2HF_3]^+$ has shown no correlation with $[(C_2H_2F_2)_3C_2HF_2]^+$ (m/z=255) and has shown about the same dependency on $(C_2H_2F_2)_4^+$ ions. This tendency indicates that the $[(C_2H_2F_2)_2C_2HF_3]^+$ is produced by the loss of C_2H_2F radical from the $(C_2H_2F_2)_4^+$.

Conclusion

The intracluster ion/molecule reactions provide a feasible

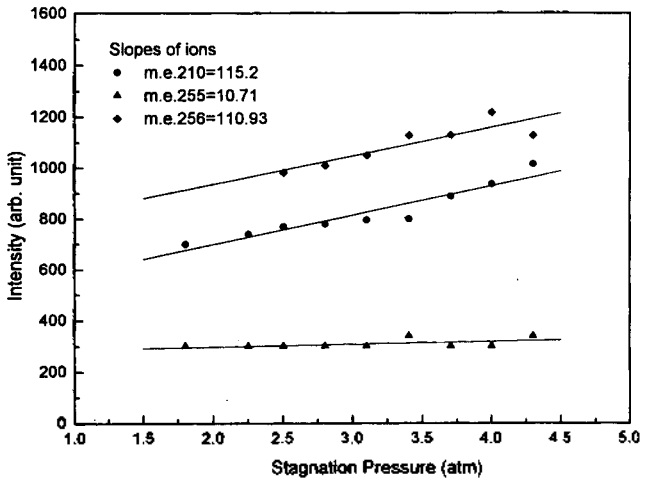

Figure 6. The intensities of the $[(C_2H_2F_2)_2C_2HF_3]^+$ (m/e=210), $[(C_2H_2F_2)_3C_2HF_2]^+$ (m/e=255), and $(C_2H_2F_2)_4^+$ (m/e=256) as a function of the stagnation pressure.

and valuable information for the understanding of the ionic polymerization mechanism. In the cationic polymerization processes we illustrate the F-shift reactions which lead to the energetically stable structure. The H-shift reactions, on the other hand, are found to be an energetically unstable process in 1,1-DFE clusters through the PM3 semi-empirical calculation. From the energy dependences on the fragmentation in the trimer and tetramer, we have proved the necessity of the additional energy. The additional energy is required for the reopening of the cyclic parent molecules as the initial step of fragmentation. The structures of the trimer and tetramer ions are predicted to be the stable six membered ring conformation whose bulky substituents will be in the equatorial positions and the relatively smaller groups are found in the axial position. Since these conformations have the steric hindrance of 1,3-axial substituents, the fragmentation occurs in 1,3-axial positions at first. In the trimer and tetramer, the major fragment species are not methyl or substituted methyl groups but HF or F atom unlike the dimer. This demonstrates that the trimer and tetramer ions are in the stable six membered ring structure.

The base peak of the tetramer, $[(C_2H_2F_2)CHF_3]^+$ m/z=210, is produced by the loss of C_2H_3F radical from the parent tetramer molecule ions. This is interpreted as the variation of the intensity with stagnation pressure.

Acknowledgment. The authors gratefully acknowledge the Korea Science and Engineering Foundation for helping the maintenance of the equipments by the Capital Equipment Grant-1995-1997.

References

1. Coolbaugh, M. T.; Vaidyanathan, G.; Peifer, W. R.; Garvey, J. F. *J. Phys. Chem.* **1991**, *95*, 8337-8343.
2. El-Shall, S. M.; Marks, C. *J. Phys. Chem.* **1991**, *95*, 4932-4935.
3. Coolbaugh, M. T.; Whitney, S. G.; Vaidyanathan, G.; Garvey, J. F. *J. Phys. Chem.* **1992**, *96*, 9139-9144.
4. Coolbaugh, M. T.; Vaidyanathan, G.; Garvey, J. F. *Int.*

Rev. Phys. Chem. **1994**, *13*, 1-19.
5. Coolbaugh, M. T.; Garvey, J. F. *Chem. Soc. Rev.* **1992**, *21*, 163-169.
6. Kappes, M.; Leutwyler, S. In *Atomic and Molecular Beam Methods*; Scoles, G., Ed.; Oxford University Press: New York, 1988; Vol 1, Chapt. 15.
7. Castleman, Jr., A. W.; Mark, T. D. In *Gaseous Ion Chemistry and Mass Spectrometry*; Furtrell, J. H., Ed.; Wiley Interscience: New York, 1986.
8. Jung, K. W.; Choi, S.-S.; Jung, K.-H. *Bull. Korean Chem. Soc.* **1992**, *13*, 306-311.
9. Choi, C. J.; Jung, K. W.; Kang, W. K.; Youn, D. Y.; Jung K.-H.; Kim, D. *Org. Mass Spectrom.* **1993**, *28*, 931-939.
10. Castleman, Jr., A. W.; Keesee, R. G. *Acc. Chem. Res.* **1986**, *19*, 413-419.
11. Garvey, J. F.; Bernstein, R. B. *J. Am. Chem. Soc.* **1987**, *109*, 1921-1934.
12. Coolbaugh, M. T.; Peifer, W. R.; Garvey, J. F. *J. Am. Chem. Soc.* **1990**, *112*, 3692-3693.
13. Castleman, Jr., A. W.; Keesee, R. G. *Chem. Rev.* **1986**, *86*, 589-618.
14. Shin, D. N.; Jung, K. W.; Jung, K.-H. *J. Am. Chem. Soc.* **1992**, *114*, 6926-6928.
15. Lee, S. Y.; Shin, D. N.; Cho, S. G.; Jung, K.-H. *J. Mass Spectrom.* **1995**, *30*, 969-976.
16. Chambers, R. D. In *Fluorine in Organic Chemistry*; Olah, G. A., Ed.; A Wiley-Interscience Press: New York 1973; Chapt. 7.
17. Jung, K. W.; Choi, C. J.; Kim, Y. S.; Jung K.-H.; Kim, D. *Int. J. Mass Spectrom. Ion Processes*, **1994**, *135*, 119-128.
18. Ceyer, S. T.; Tiedemann, P. W.; Ng, C. Y.; Mahan, B. H.; Lee, Y. T. *J. Chem. Phys.* **1979**, *70*, 2138-2143.
19. Shioharo, H.; Sato, H.; Washida, N. *J. Phys. Chem.* **1990**, *94*, 6718-6723.
20. Stewart, J. J. P. *J. Comp. Chem.* **1989**, *10*, 209-220.
21. Stewart, J. J. P. *Quantum Chemistry Program Exchange*, 1993.
22. O'Malley, R. M.; Jennings, K. R. *Int. J. Mass Spectrom. Ion Processes*; **1973**, *11*, 89-98.
23. Buck, U.; Meyer, H. *Surf. Sci.* **1985**, *156*, 275.

Effect of a Nonionic Surfactant on the Adsorption and Kinetic Mechanism for the Hydrolysis of Microcrystalline Cellulose by Endoglucanase I and Exoglucanase II

Dong Won Kim*, Young Hun Jang, Young Kyu Jeong, and Ki Hyang Son

Department of Chemistry, College of Natural Sciences, Chungbuk National University, Cheongju 361-763, Korea
Received November 26, 1996

Effect of a nonionic surfactant, Tween 20 on the adsorption and kinetic mechanism for the hydrolysis of a microcrystalline cellulose, Avicel PH 101, by endoglucanase I (Endo I) and exoglucanase II (Exo II) isolated from *Trichoderma viride* were studied. The Langmuir isotherm parameters, amount of maximum adsorption (A_{max}) and adsorption equilibrium constant (K_{ad}) for the adsorption, were obtained in the presence and the absence of nonionic surfactant. On the addition of Tween 20, the K_{ad} and A_{max} values of Exo II were decreased, while those of Endo I were not affected. These indicate that the adsorption affinity of Exo II on the cellulose is weakened by nonionic surfactant, and the surfactant enhanced desorption of Exo II from insoluble substrate. The enzymatic hydrolysis of the cellulose can be described by two parallel pseudo-first order reactions using the percentages of easily (C_a) and hardly (C_b) hydrolyzable cellulose in Avicel PH 101 and associated rate constants (k_a and k_b). The C_a value was increased by adding Tween 20 for all enzyme samples (Exo II, Endo I and their 1 : 1 mixture) implying that the low-ordered crystalline fraction in the cellulose may be partly dispersed by surfactant. The k_a value was not affect by adding Tween 20 for all enzyme samples (Exo II, Endo I and their 1 : 1 mixture). The k_b value of Exo II was increased by adding Tween 20, while that of Endo I was not affected. This suggests that the surfactant helps the Exo II desorb from microcrystalline cellulose, and increase the hydrolysis rate. These results were show that the increase of hydrolysis of cellulose by the nonionic surfactant is due to both the activation of Exo II and partial defibrillation of the cellulose.

Introduction

The enzymatic degradation of cellulose is catalyzed by three classes of enzymes: endoglucanases, exoglucanases, and β-glucosidase working in a synergistic way.[1,2] The multiplicity of the cellulases, the structural complexity of cellulosic materials, and product inhibition cause the difficulty in the elucidation of the hydrolysis mechanism.

The adsorption of cellulase on the cellulose is very important because adsorption is a prerequisite step in the en-

*Corresponding Author